

## SUPPLEMENTARY MATERIALS

### Strain softening and stiffening responses of spider silk fibers probed using Micro-Extension Rheometer

Sushil Dubey<sup>†</sup>, Chinmay Hemant Joshi<sup>§§</sup>, Sukh Veer<sup>†§</sup>, Divya Uma<sup>#</sup>,  
Hema Somanathan<sup>§</sup>, Sayantan Majumdar<sup>†</sup>, and Pramod A Pullarkat<sup>†\*</sup>

<sup>†</sup> *Soft Condensed Matter Group, Raman Research Institute,  
C. V. Raman Avenue, Bengaluru, Karnataka 560 080, India*

<sup>§</sup> *IISER TVM Centre for Research and Education in Ecology and Evolution (ICREEE),  
School of Biology, Indian Institute of Science Education and Research,*

*Thiruvananthapuram, Kerala 695 551, India*

<sup>#</sup> *School of Liberal Studies, Azim Premji University, Bengaluru, Karnataka 560 100, India*

---

\* Corresponding author: pramod@rri.res.in; <sup>§</sup>These authors contributed equally.

## I. EXTRACTION OF SILK FOR FORCE MEASUREMENT

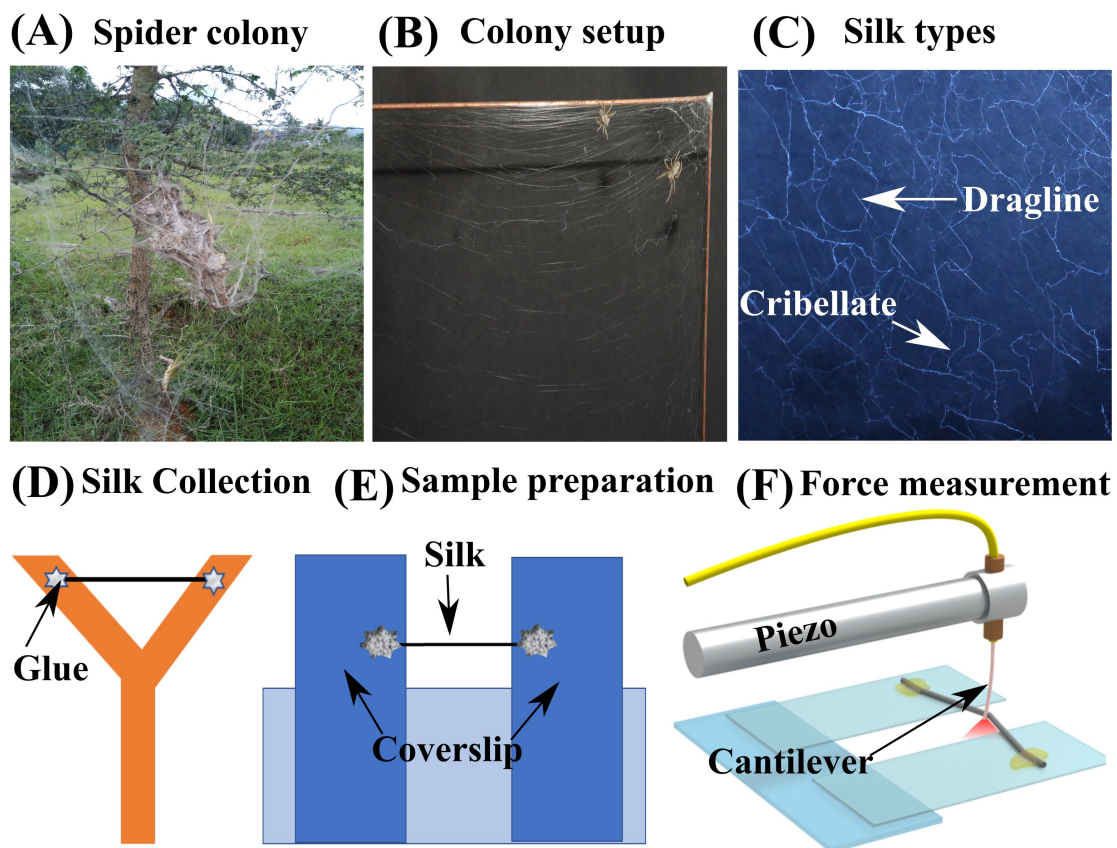


Fig. S1. (A) Photograph of a web of social spider *Stegodyphus sarasinorum* in the wild. (B) Photograph of spiders with their web built on a metal wire frame as detailed in the Material and Methods. (C) Image showing an expanded view of the web with dragline and cribellate silk indicated by the labels. (D) Schematic of a silk strand transferred to a Y-shaped cardboard frame. (E) Schematic of the silk strand after it has been transferred to a frame made of two coverslips attached to a glass slide. (F) Schematic of the a silk fiber stretched using an optical fiber cantilever attached to piezo.

## II. IMAGES OF SILK BEING PULLED USING OPTICAL FIBER

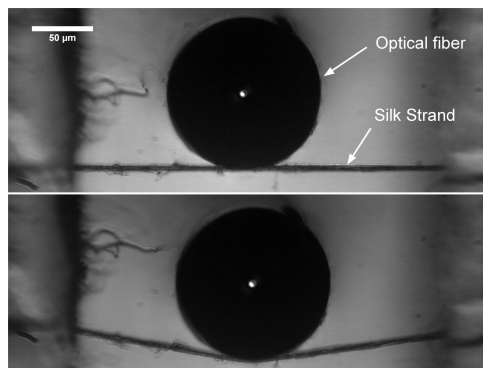


Fig. S2. A typical images of a silk strand which is stretched using an optical fiber in transverse direction. Images of silk strand before pulled (top) and after pulled (bottom). The bright spot is laser light exiting the core of the optical fiber which is detected using a Position Sensitive Detector (PSD).

## III. A PHOTOGRAPH OF THE MICRO-EXTENSION RHEOMETER

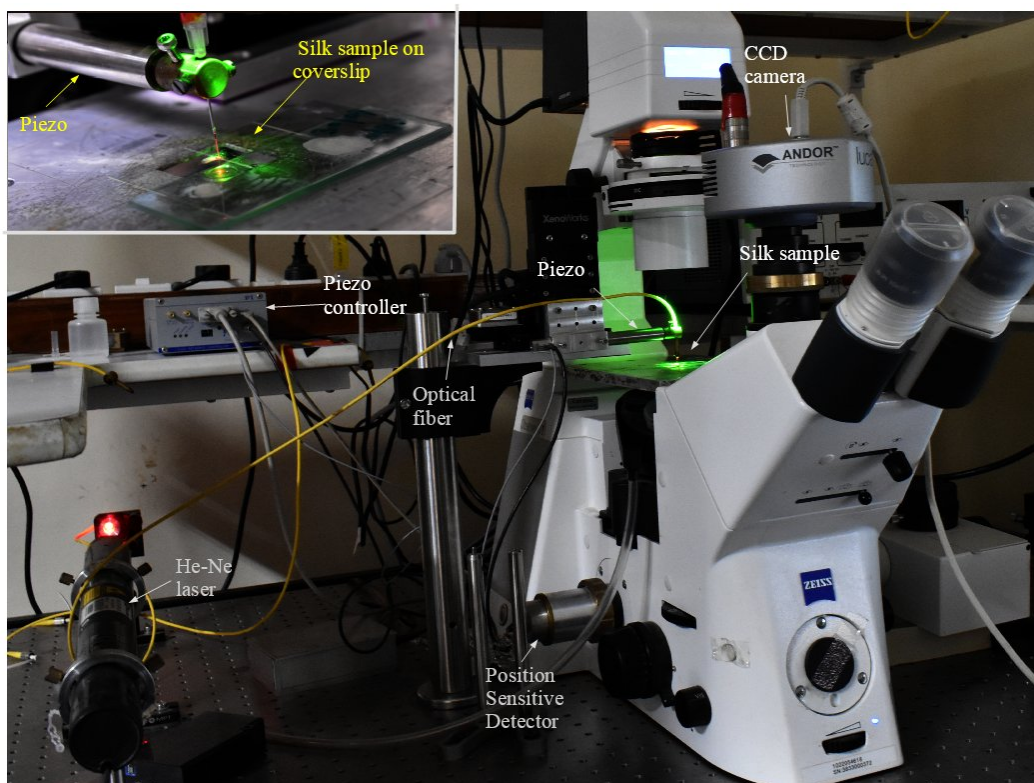


Fig. S3. Photograph of the optical fiber based force apparatus Micro-Extension Rheometer (MER) used to investigate the mechanical properties of spider silk. The piezo drive and the Position Sensitive Detector (PSD) are interfaced to a computer to operate the setup in a feedback strain control mode. More details are described in the main text. The inset shows the close up view of the sample which is being pulled with the optical fiber.

## IV. ELECTRON MICROSCOPY IMAGES OF DRAGLINE AND CRIBELLATE SILK

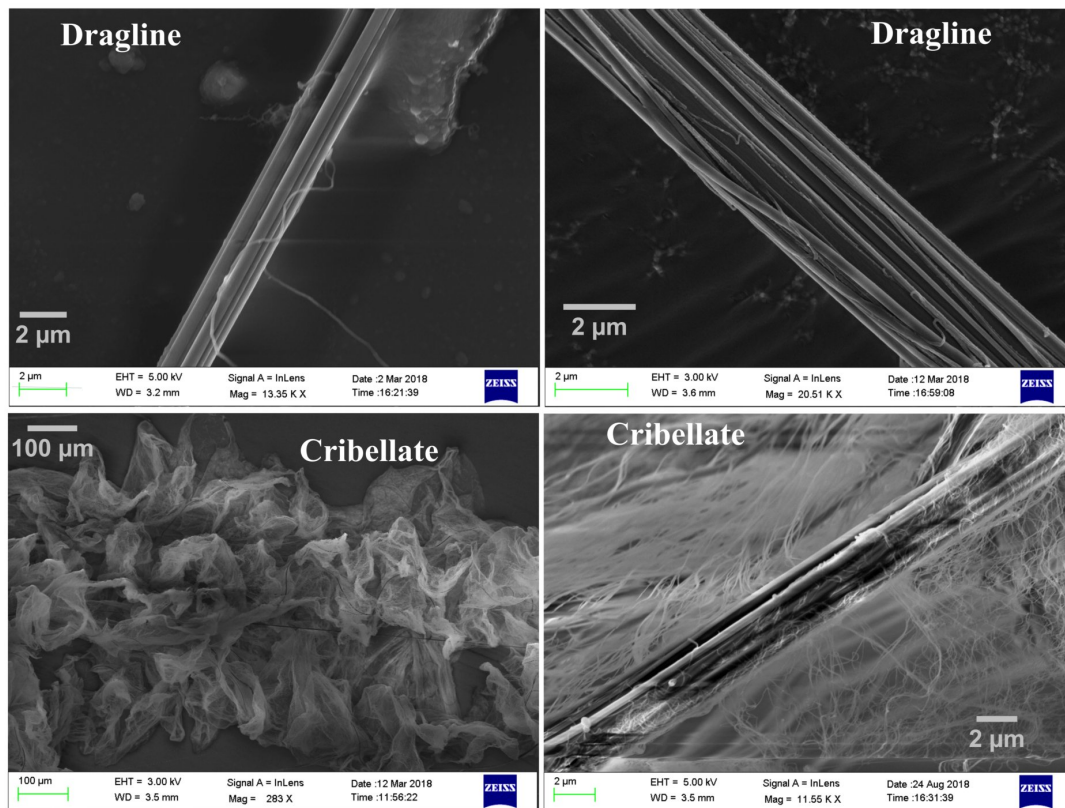


Fig. S4. Electron Microscopy images of dragline and cribellate silk: Dragline is made of many thin fibers whereas cribellate consist of a central fiber and surrounded by ultrathin fibers which are sticky in nature.

## V. CANTILEVER CALIBRATION TEST

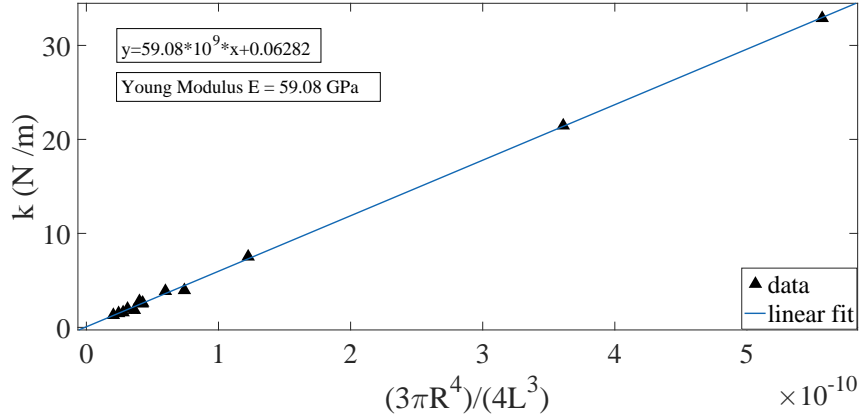


Fig. S5. Calibration test of optical fiber by hanging known weights of metal wires on optical fiber. The force constant is given by  $k = \frac{3\pi ER^4}{4L^3}$ , where  $R$  is the radius, and  $L$  is the length of the optical fiber. The data is fitted to a straight line (parameters shown in the figure). The slope gives the Young's modulus.

## VI. PRE-TENSION FOR DIFFERENT SILK STRANDS

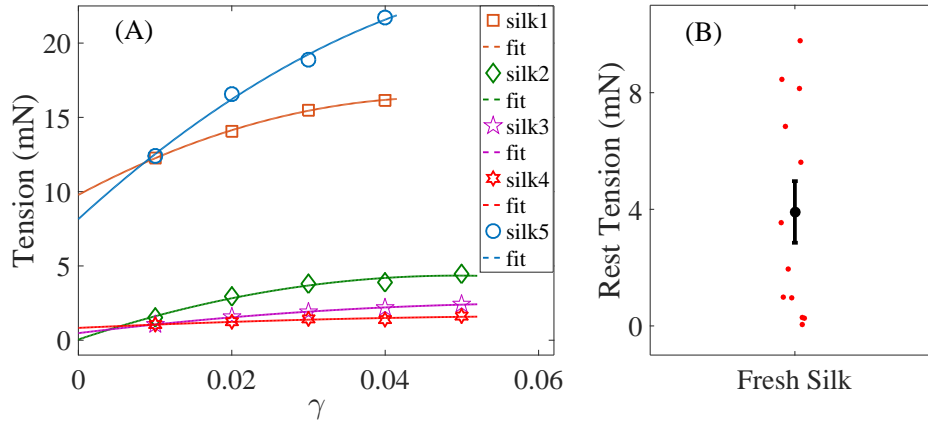


Fig. S6. The silk strands are under pre-tension when they are in the web. (A) This pre-tension is obtained by extrapolating the steady state tension vs. strain to zero strain by fitting the data with the equation  $(-ax^2 + bx + c)$ . Fits for different silk strands are shown. (B) Pre-tension values for different silk strands (red dots) (The black dot and the error bar are the mean and standard error, respectively).

## VII. FOURIER TRANSFORM ANALYSIS

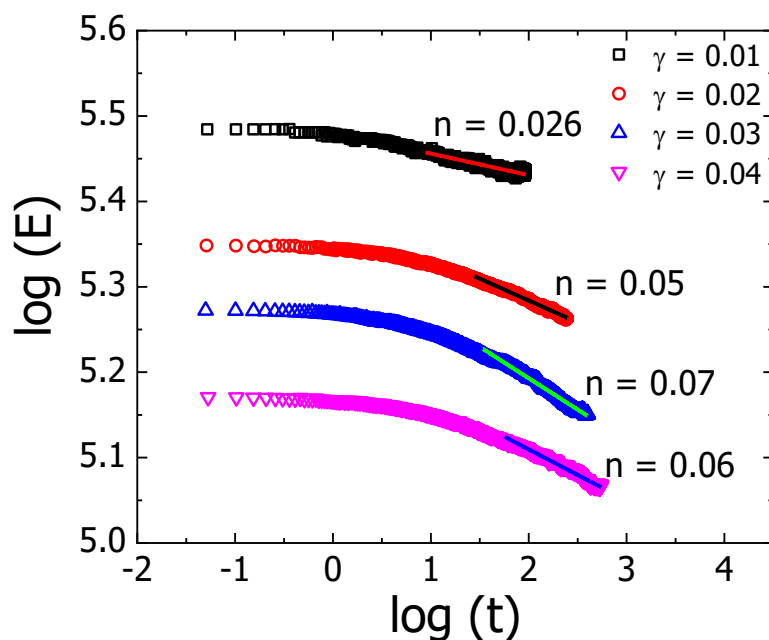


Fig. S7. Variation of stress relaxation modulus  $E$  (defined in the main text) as a function of time. For convenience, logarithm of the quantities are shown. The magnitudes of the logarithmic slope  $n$  (described in the main text) are indicated in the figure for different applied step-strain values.

## VIII. NORMALISED MODULUS IN LARGE STRAIN REGIME

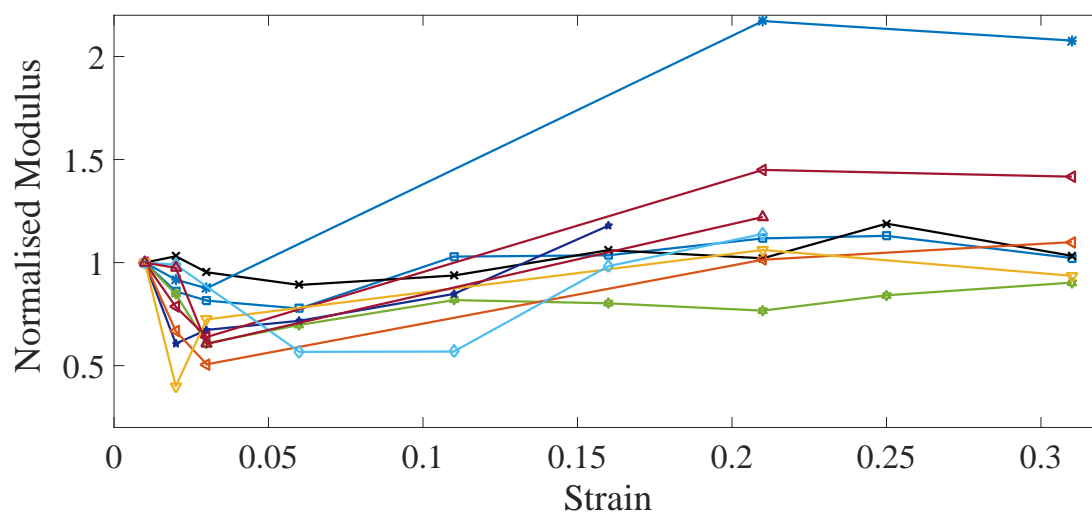


Fig. S8. Elastic modulus normalised with respect to its initial value shows that there is an initial softening.

## IX. RAMP EXP

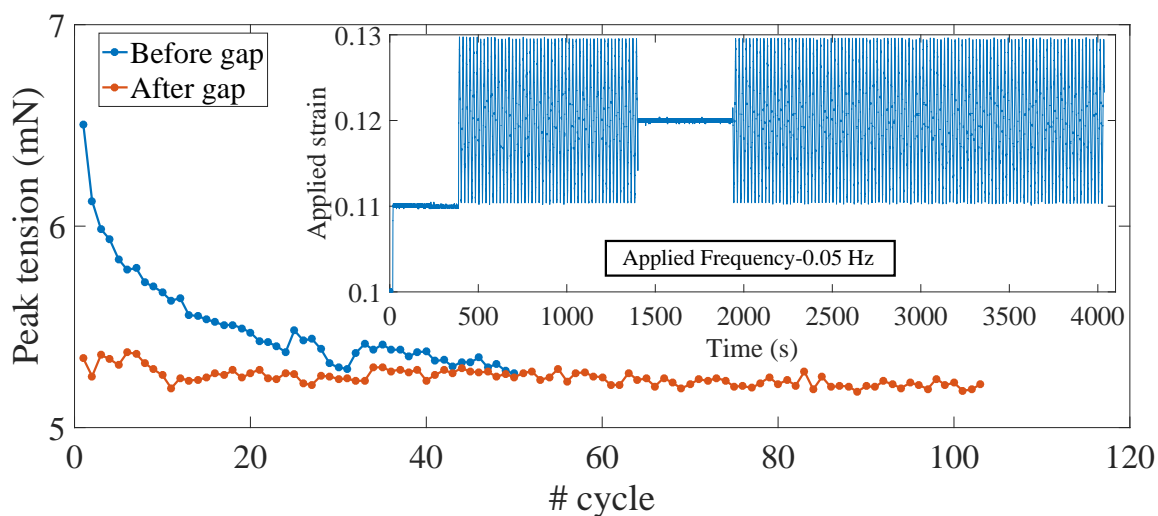


Fig. S9. Variation in peak tension with cycle number obtained from superimposed triangular wave soon after a strain step (blue dots) and that obtained after a wait time without superimposed triangular wave (orange dots). This data shows that the silk fiber reaches a limit cycle after approximately 50 cycles.

## X. TENSION AND MODULUS RESPONSE OF PROTEIN UNFOLDING-REFOLDING MODEL

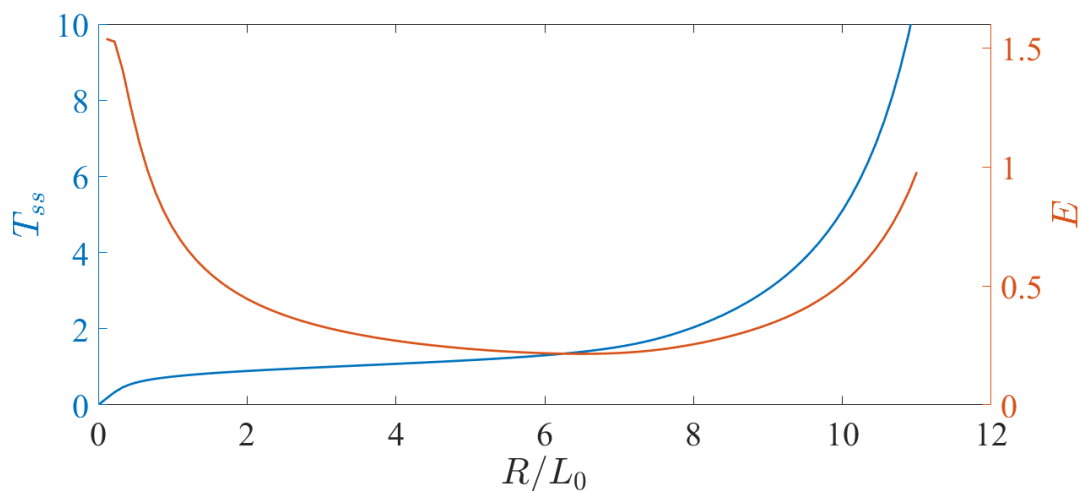


Fig. S10. Equilibrium tension and Young's modulus versus extension curves for a structure containing spectrin molecules with domains that can unfold and refold in a force dependent manner. The Young's modulus shows strain softening followed by stiffening response. The stiffening occurs when most of the domains are in the unfolded state and the molecules behave as a WLC.  $T_{ss}$  is the steady state tension,  $E$  is the Young's modulus,  $R$  is the spectrin end to end distance and  $L_0$  is contour length. (REF: Dubey *et al.* 2019 BioRxiv: 510560).

## XI. ULTRASTRUCTURE OF SILK

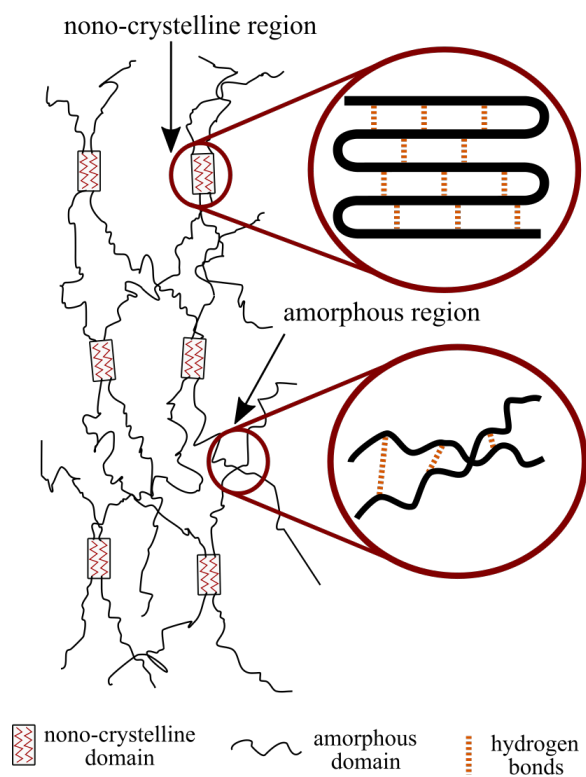


Fig. S11. A schematic of the ultrastructure of dragline silk showing the two types of domains—namely, nano-crystalline and amorphous regions as indicated in the figure. The red dotted lines represent hydrogen bonds.